Medicinal Chemistry Research
https://doi.org/10.1007/s00044-020-02640-2

MEDICINAL CHEMISTRY RESEARCH

ORIGINAL RESEARCH

# First in class (*S*,*E*)-11-[2-(arylmethylene)hydrazono]-PBD analogs as selective CB2 modulators targeting neurodegenerative disorders

David Mingle[1] · Meirambek Ospanov[2] · Mohamed O. Radwan[3,4,5] · Nicole Ashpole[6] · Masami Otsuka[3,4] · Samir A. Ross[2,6] · Larry A. Walker[2] · Abbas G. Shilabin[1] · Mohamed A. Ibrahim[2,5]

Received: 4 August 2020 / Accepted: 22 September 2020


## Abstract

Newly designed pyrrolo[2,1-c][1,4]benzodiazepines tricyclic skeleton has shown potential clusters of cannabinoid receptors CB1/CB2 selective ligands. CB2 plays a critical role in microglial-derived neuroinflammation, where it modulates cell proliferation, migration, and differentiation into M1 or M2 phenotypes. Beginning with computer-based docking studies accounting the recently discovered X-ray crystal structure of CB2, we designed a series of PBD analogs as potential ligands of CB2 and tested their binding affinities. Interestingly, computational studies and theoretical binding affinities of several selected (*S*,*E*)-11-[2-(arylmethylene)hydrazono]-PBD analogs, have revealed the presence of potential selectivity in binding attraction toward CB1 and CB2. Reported here is the discovery of the first representatives of this series of selective binding to CB2. Preliminary data showed that this class of molecules display potential binding efficacy toward the cannabinoid receptors tested. Intriguingly, initial cannabinoid binding assay showed a selective binding affinity of **4g** and **4h** showed $K_i$ of 0.49 and 4.7 μM toward CB2 receptors while no binding was observed to CB1. The designed leads have shown remarkable stability pattern at the physiological pH magnifying their therapeutic values. We hypothesize that the PBD tricyclic structure offers the molecule an appropriate three-dimensional conformation to fit snugly within the active site of CB2 receptors, giving them superiority over the reported CB2 agonists/inverse agonists. Our findings suggested that the attachment of heterocyclic ring through the condensation of diazepine hydrazone and S- or N-heterocyclic aldehydes enhances the selectivity of CB2 over CB1.

## Graphical Abstract

First in class (*S*,*E*)-11-[2-(Arylmethylene)hydrazono]-PBD analogs as Selective CB2 modulators Targeting Neurodegenerative Disorders

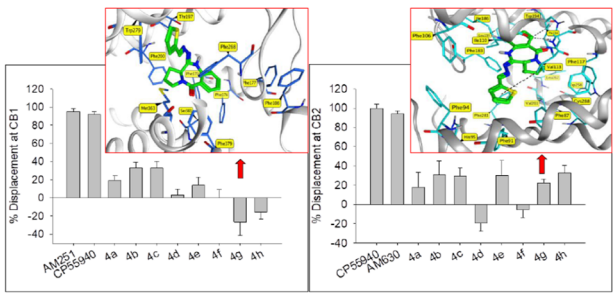


These authors contributed equally: Abbas G. Shilabin, Mohamed A. Ibrahim

**Supplementary information** The online version of this article (https://doi.org/10.1007/s00044-020-02640-2) contains supplementary material, which is available to authorized users.

✉ Abbas G. Shilabin
shilabin@etsu.edu

✉ Mohamed A. Ibrahim
mmibrahi@olemiss.edu

Extended author information available on the last page of the article

Published online: 04 October 2020

**Keywords** Cannabinoid receptors CB1/CB2 · Pyrrolobenzodiazepines · Neuroinflammation · Neurodegenerative diseases · Central nervous system (CNS)

**Abbreviations**

| | |
|---|---|
| CB2 | Cannabinoid Receptor Subtype 2 |
| PBD | Pyrrolo[2,1-c][1,4]benzodiazepines |
| AD | Alzheimer's Disease |
| PA | Parkinson's Disease |
| THC | Tetrahydrocannabinol |
| CBN | Cannabinol |

## Introduction

Neurodegenerative diseases are characterized by slow progressive loss of neurons in the central nervous system (CNS), which are associated with altered proteins that deposit in the human brain and peripheral organs leading to deficits in certain brain functions (e.g., movement, memory, cognition) performed by the affected CNS region [1]. The progression of many neurodegenerative diseases is thought to be driven by misfolding, seeded aggregation and cell–cell transmission of disease-related proteins, leading to the successive spreading of pathological protein aggregates [2]. The mechanism(s) underlying their progressive nature remains unclear. Neurodegenerative diseases include Parkinson's disease (PD), amyotrophic lateral sclerosis (ALS), multiple sclerosis, Alzheimer's disease (AD), Huntington's disease, and multiple system atrophy. The shortfall in movement is named ataxia, while shortfall in mental functioning is named dementia which is accountable for the major problem of neurodegenerative diseases [3]. The endogenous cannabinoid system consists of two receptors subtype 1 (CB1) and subtype 2 (CB2), seven endocannabinoid ligands (Fig. 1) [4], and several proteins that regulate the endocannabinoid metabolic pathways [5, 6]. Modulating the activity of the endocannabinoids system demonstrated therapeutic promise in a wide range of diseases [7]. The cannabinoid receptors subtype 2 (CB2), that were identified molecularly in 1993, have shown promising therapeutic potential for treating various diseases with no adverse psychotropic effects that are commonly associated with CB1 receptor–based therapies which hamper the development of direct-acting CB1 agonists [8].

CB2 receptors are representing novel targets to develop new therapeutic approaches and developed positron emission tomography (PET) probes to early diagnose neuroinflammation in several neurodegenerative disorders such as PD and AD [9]. CB2 is localized in the peripheral immune system and overexpressed in response to neuroinflammation, while CB1 is present in the CNS [10]. Many studies have investigated the relation between chronic neuroinflammation and CB2 upregulation in pain [11] and inflammation animal models [12]. Interestingly, CB2 agonists show potential ability to reduce inflammation, tau protein hyperphosphorylation and oxidative stress, and induce Aβ clearance leading to cognitive improvement in AD models. Several established models have strengthened the proof of concept, the natural CB2 agonist, β-caryophyllene (BCP), showed favorable neuroprotective effect in a rotenone (ROT)-induced animal model of PD [13]. Administration of MDA7 reduces the neuroinflammation and amyloid deposition while reinstates the hippocampal synaptic plasticity in rats [14].

Another CB2 agonist, JWH-133, showed ability to attenuate hippocampal microglial stimulation, amyloid aggregation in transgenic mice models of AD [15–18].

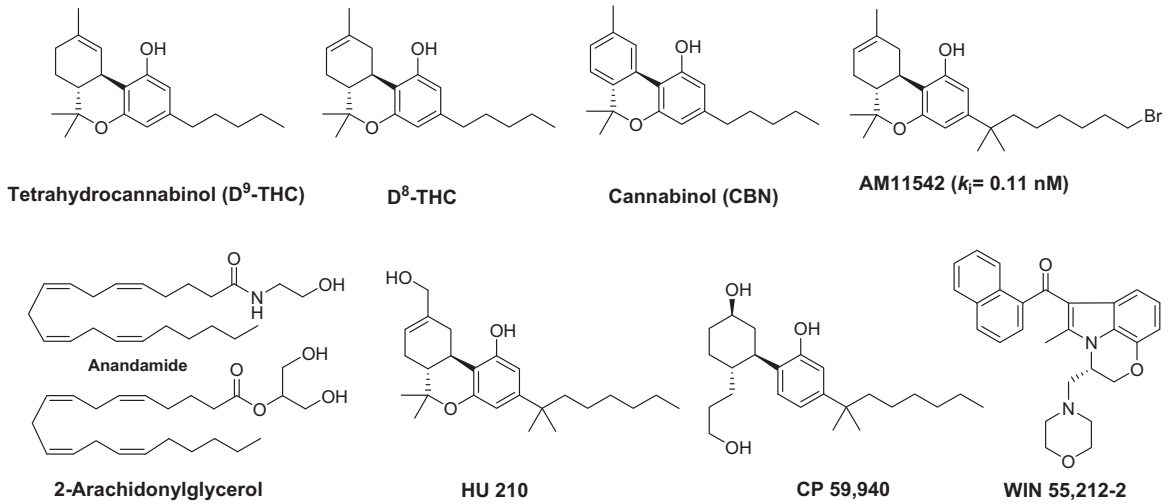


**Fig. 1** Structures of various natural and synthetic cannabinoid ligands

Knockout of CB2 receptor enhances the solubility of Aβ42/Aβ40 and plaque/cortical deposition in brain of J20 mice [15, 16]. The potentiality of CB2 agonists as neuroprotective agents have been polished by the absence of psychotropic adverse effects generally seen with CB1 agonists [17].

In 2018, Sharon Anavi-Goffer and Juerg Gertsch have patented CB2R inverse agonists for treating or ameliorating psychiatric disorders [18]. Parallel discovery approach using high throughput screening of a library of 640 FDA-approved drugs as potential CB2 ligands has led to the identification of the CB2 inverse agonist, raloxifene, which has been approved to treat post-menopausal. Despite the increasing number of discovered CB2 agonists, few synthetic members have made it to clinical trials; the CB2R agonists such as CP55940, and JTE-907 have completed phase II for the pain therapy but none of them has been used in neurodegenerative diseases which represents variation between preclinical and clinical data that promotes further exploration.

Pyrrolo[2,1-c][1,4]benzodiazepines (PBDs) are a class of natural products, known to possess anti-tumor and antibiotic activities [19]. We hypothesize that the PBD tricyclic structure offers the molecule an appropriate three-dimensional conformation to fit snugly within the active site of CB receptors, enabling them to interfere with the endocannabinoid signaling system and giving them superiority over the reported CB2 agonists/inverse agonists.

This work is the first study of the novel class of PBD-11-hydrazinyl derivatives through a structure-based rational design using a multi-step synthesis approach to establish potential clusters of selective CB ligands. Our preliminary results including in vitro cannabinoid receptor binding data supported the potentiality of the proposed synthetic analogs as CB1/CB2 potent selective ligands. Beginning with computer-based docking studies, calculation of ADMET, and physicochemical properties, we attempted to elaborate a series of PBD analogs as potential ligands of CB2 and tested their binding affinities. We have considered the calculation of blood brain barrier penetration and retention (BBB filter and LogBB) in silico using ADMET predict 9 from Simulation Plus, Inc., which predicts the possible metabolites of our lead compounds through Site-of-metabolism models considering Phase I and Phase II metabolism, which is crucial in understanding toxicities.

## Material and methods

### General experimental procedures

The $^{1}H$ and $^{13}C$ NMR spectra were recorded in DMSO-$d_6$ and $CDCl_3$ on a JEOL-NMR Eclipse-400 MHz spectrophotometer operating at 400 MHz for $^{1}H$ and 100 MHz for $^{13}C$ NMR. Chemical shift ($\delta$) values are presented in ppm and in reference to the residual solvent signals of DMSO-$d_6$ and $CDCl_3$ at $\delta_H/\delta_C$ 2.50/39.5 and 7.25/70.2, respectively. The coupling constants value (J) reported in Hz. Genesis II FT-IR spectrometer was also used for all IR spectra. Melting points was measured using a Thermo Scientific Electrothermal Digital Melting Point Apparatus IA9100 series. UV/Vis. absorbance measurements were recorded on Agilent Technologies Cary 8454 UV/Vis. spectrophotometer with a PCB-1500 water Peltier circulating system. Optical rotations were measured on Roudolph Research Analitical AUTOPOL® III polarimeter. HRESIMS data were acquired using a Bruker BioApex-FTMS with electrospray ionization (ESI).

Other common chromatographic techniques such as thin layer chromatography on precoated silica gel $G_{254}$ aluminium plates and silica gel flash column chromatography were also engaged in the purification of the synthesized compounds.

### General method for synthesis of (S,E)-11-[2-(arylmethylene) hydrazono]-pyrrolo[2,1-c][1,4]benzodiazepinem (4a–4h)

To a solution of **3** (691 mg, 3.0 mmol) in anhydrous methanol (20 mL) was added aldehyde (10 mmol). 3 A° molecular sieves (2.0 g) was also added and stirred at room temperature. Various modifications were used to obtain compounds **4a–4h**.

### (S,E)-11-[2-(phenylmethylene)hydrazono]-pyrrolo[2,1-c] [1,4]benzodiazepinem (4a)

Starting material benzaldehyde (1.02 mL, 10 mmol) was used and the reaction mixture was stirred under nitrogen gas overnight for 15 h. Extraction was performed using chloroform/isopropanol (2:1) (3 × 20 mL), where the organic layers were dried over anhydrous $Na_2SO_4$. The solvent mixture was then removed in vacuo and washed with diethyl ether, filtered off and dried to afford an off-white solid of **4a**. The final product was purified using crystallization from isopropanol to yield colorless needle-shaped crystals. Yield 688 mg (72.0%); mp 198–200 °C; $[\alpha]^{25}_D = +50°$ (*c* 0.5, $CHCl_3$); $^{1}H$-NMR (400 MHz, $CDCl_3$): δ = 2.02–2.07 (m, 3H), 2.98–3.02 (m, 1H), 3.65–3.71 (m, 1H), 3.78–3.82 (m, 1H), 4.37 (d, *J* = 6.2 Hz, 1H, H-11a), 6.99 (d, *J* = 8.1 Hz, 1H), 7.16 (t, *J* = 7.1 Hz, 1H), 7.43 (s, 4H), 7.77–7.80 (m, 2H), 7.96 (d, *J* = 8.01 Hz, 1H), 8.48 (s, 1H, CH), 8.53 (s, 1H, NH); $^{13}C$-NMR (100 MHz, $CDCl_3$): δ = 23.6, 26.2, 47.4, 55.5 (C-11a), 120.8, 123.9, 126.4, 128.2, 128.9, 130.9, 131.5, 132.5, 134.6, 136.8, 157.6, 157.8, 166.1 (CO); UV $\lambda_{max}$ (MeOH): 223, 319; IR (neat): 3351, 2981, 2879, 2370, 1963, 1710, 1627 (C=O), 1471, 1400, 1295, 1097, 964, 831, 757, 692, 630; GC-MS (70 eV) *m/z* (%): 318 (25) [M+], 241 (100), 172 (9), 145 (16), 119

(13), 90 (10), 70 (13); HRMS m/z calcd for $C_{19}H_{18}N_4O$ $[M + H]^+$ 319.1559, found 319.1612.

### (S,E)-11-[2-(4-ethylphenyl-methylene)hydrazono]-pyrrolo [2,1-c][1,4]benzodiazepine (4b)

Starting material benzaldehyde (1.34 mL, 10 mmol) was used and the reaction mixture was stirred under nitrogen gas overnight for 15 h. Evaporation of solvent mixture was carried out under vacuum. Crystallization of the compound was achieved with n-pentane to give a yellow solid rod-shaped crystal of compound **4b**. Yield 732 mg (70.4%); mp 168–170 °C; $[\alpha]^{25}_D = +54°$ (*c* 0.5, $CHCl_3$); $^1$H-NMR (400 MHz, $CDCl_3$): 1.26 (t, $J = 7.7$ Hz, 3H), 1.99–2.15 (m, 3H), 2.69 (q, $J = 7.7$ Hz, 2H), 2.98–2.99 (m, 1H), 3.64–3.73 (m, 1H), 3.78–3.84 (m, 1H), 4.38 (d, $J =$ 5.5 Hz, 1H), 7.00 (d, $J = 7.3$ Hz, 1H), 7.17 (t, $J = 8.1$ Hz, 1H), 7.26 (d, $J = 8.6$ Hz, 1H), 7.43 (t, $J = 7.7$ Hz, 1H), 7.71 (d, $J = 8.2$ Hz, 2H), 7.97 (d, $J = 9.5$ Hz, 1H), 8.46 (s, 1H), 8.52(s,1H); $^{13}$C-NMR (100 MHz, $CDCl_3$): $\delta = 15.5$, 23.6, 26.2, 29.0, 47.4, 55.5 (C-11a), 120.7, 126.4, 128.3, 128.4, 131.5, 132.1, 132.5, 136.9, 147.6, 157.3, 157.7, 166.1 (C=O); UV $\lambda_{max}$ (MeOH): 224, 322; IR (neat): 3733, 3598, 3343, 3261, 2966, 2873, 2360, 2341, 1625 (C=O), 1469, 1396, 1270, 1160, 970, 831, 752, 669; GC-MS (70 eV) *m/z* (%): 403 (1) [M+], 346(32), 241 (100), 207 (9), 172 (8), 145 (14), 119 (12), 90 (8), 70 (11), 44 (4); HRMS m/z calcd for $C_{21}H_{22}N_4O$ $[M + H]^+$ 347.1872, found 347.1930.

### (S,E)-11-[2-(4-methoxyphenylmethylene)hydrazono]-pyrrolo[2,1-c][1,4]benzodiazepine (4c)

Starting material 4-methoxybenzaldehyde (1.22 mL, 10 mmol) was used and the reaction mixture was stirred under nitrogen gas for 6 h. The solution was filtered off and washed with diethyl ether to afford a light yellow solid of compound **4c**. The final product was purified using crystallization from isopropanol to yield colorless needle-shaped crystals. Yield 711 mg (68%); mp 212–214 °C; $[\alpha]^{25}_D = +40°$ (*c* 0.5, $CHCl_3$); $^1$H-NMR (400 MHz, $CDCl_3$): $\delta = 1.88$–2.13 (m, 3H), 2.99–3.00 (m, 1H), 3.44–3.71 (m, 1H), 3.77–3.80 (m, 1H), 3.84 (s, 3H, $OCH_3$), 4.37 (d, $J = 8.1$ Hz, 1H, H-11a), 6.93 (d, $J = 8.1$ Hz, 2H), 6.98 (d, $J = 7.7$ Hz, 1H), 7.15 (t, $J = 7.7$ Hz, 1H), 7.42 (t, $J = 7.0$ Hz, 1H), 7.73 (d, $J = 8.8$ Hz, 2H), 7.93 (d, $J =$ 6.2 Hz, 1H), 8.42 (s, 1H, NH), 8.52 (s, 1H); $^{13}$C-NMR (100 MHz, $CDCl_3$): $\delta = 23.6$, 26.1, 47.4, 55.03 (C-11a, $CH_3$), 114.3, 120.7, 123.7, 126.3, 127.3, 129.8, 131.5, 132.5, 137.0, 157.0, 157.4, 161.8, 166.1 (CO); UV $\lambda_{max}$ (MeOH): 221, 325; IR (neat): 3259, 2958, 2854, 2350, 1706, 1619 (C=O), 1517, 1469, 1394, 1224, 1120, 927, 827, 759, 700; GC-MS (70 eV) *m/z* (%): 348 (65) [M+], 241 (100), 160 (8), 145 (10), 119 (23), 90 (10), 70 (15); HRMS m/z calcd for $C_{20}H_{20}N_4O_2$ $[M + H]^+$ 349.1665, found 349.1721.

### (S,E)-11-[2-(4-fluorophenylmethylene)hydrazono]-pyrrolo [2,1-c][1,4]benzodiazepine (4d)

Starting material 4-flurobenzaldehyde (1.07 mL, 10 mmol) was used and the reaction mixture was stirred under nitrogen gas for 4 h. This is followed by quenching the mixture with 20 mL distilled water to afford a white precipitate of **4d**. Crystallization of the final product was accomplished in hexane/acetone to yield greenish rod-shaped crystals. Yield 740 mg (73.3%); mp 205–207 °C; $[\alpha]^{25}_D = +30°$ (*c* 0.5, $CHCl_3$); $^1$H-NMR (400 MHz, $CDCl_3$): $\delta = 2.00$–2.13 (m, 3H), 2.96–2.99 (m, 1H), 3.68–3.70 (m, 1H), 3.78–3.81 (m, 1H), 4.38 (d, $J = 5.9$ Hz, 1H, H-11a), 6.99 (d, $J = 7.3$ Hz, 1H), 7.12 (t, $J = 8.8$ Hz, 2H), 7.18 (t, $J = 7.0$ Hz, 1H), 7.43 (t, $J = 6.6$ Hz, 1H), 7.78 (t, $J = 6.6$ Hz, 2H), 7.96 (d, $J =$ 6.2 Hz, 1H), 8.45 (s, 1H, CH), 8.49 (s, 1H, NH); $^{13}$C-NMR (100 MHz, $CDCl_3$): $\delta = 23.6$, 26.1, 47.4, 55.5 (C-11a), 116.0, 116.2, 120.8, 123.9, 126.5, 130.1, 130.1, 131.5, 132.5, 136.7, 156.5, 157.7, 161.8, 166.0 (C=O); UV $\lambda_{max}$ (MeOH): 222, 236, 313; IR (neat): 2348, 1710, 1625 (C=O), 1508, 1471, 1396, 1270, 1226, 1155, 833, 755, 700, 520; GC-MS (70 eV) *m/z* (%): 336 (44) [M+], 241 (100), 172 (9), 145 (19), 119 (19), 90 (10), 70 (13); HRMS m/z calcd for $C_{19}H_{17}FN_4O$ $[M + H]^+$ 337.1465, found 337.1521.

### (S,E)-11-[2-(4-pyridinemethylene)hydrazono]-pyrrolo[2,1-c] [1,4]benzodiazepine (4e)

Starting material 4-pyridinecarboxaldehyde (0.94 mL, 10 mmol) was used and the reaction mixture was stirred under nitrogen gas for 4 h. The reaction mixture was then quenched with 20 mL of distilled water and filtered off. Crystallization of the crude product was completed using pentane to afford a yellow crystalline solid of compound **4e**. Yield 606 mg (63.3%) mp 242–244 °C; $[\alpha]^{25}_D = +56°$ (*c* 0.5, $CHCl_3$); $^1$H-NMR (400 MHz, $CDCl_3$): $\delta =$ 1.88–2.13 (m, 3H), 2.97–2.98 (m, 1H), 3.67–3.71 (m, 1H), 3.79–3.84 (m, 1H), 4.38 (d, $J = 5.8$ Hz, 1H, H-11a), 7.02 (d, $J = 8.0$ Hz, 1H), 7.20 (t, $J = 7.3$ Hz, 1H), 7.45 (t, $J =$ 8.1 Hz, 1H), 7.63 (d, $J = 4.8$ Hz, 2H, py), 7.97 (d, $J =$ 8.0 Hz, 1H), 8.44 (s, 1H, CH), 8.50 (s, 1H, NH), 8.68 (d, $J = 4.8$ Hz, 2H, py); $^{13}$C-NMR (100 MHz, $CDCl_3$): $\delta =$ 23.6, 26.2, 47.43, 55.5 (C-11a), 120.9, 121.8, 124.3, 126.7, 131.5, 132.6, 136.3, 141.7, 150.5, 155.4, 158.9, 165.9 (C=O); UV $\lambda_{max}$ (MeOH): 223, 334; IR (neat): 3276, 2977, 2879, 2360, 2341, 1625 (C=O), 1585, 1400, 1220, 1097, 991, 755, 530; GC-MS (70 eV) *m/z* (%): 319 (14) [M+], 281(4), 241 (100), 207 (9), 172 (11), 145 (16), 119 (12),

90 (11), 70 (15), 44 (4); HRMS m/z calcd for $C_{18}H_{17}N_5O$ $[M + H]^+$ 320.1511, found 320.1566.

#### (S,E)-11-[2-(4-(4-formylphenyl)morpholinemethylene) hydrazono]-pyrrolo[2,1-c][1,4]benzodiazepine (4f)

Starting material 4-(4-Formylphenyl)morpholine (1910 mg, 10 mmol) was used and the reaction mixture was stirred under nitrogen gas overnight for 15 h. The crude product was subjected to flash column chromatography using hexane/acetone (1:1) and the solvent was evaporated in vacuo. Crystallization of the compound was performed from pentane to afford yellow rod-shaped crystals of compound **4f**. Yield 629 mg, (52.0%); mp 198–200 °C; $[\alpha]^{25}_D = +46°$ (*c* 0.5, $CHCl_3$); $^1$H-NMR (400 MHz, $CDCl_3$): δ = 1.99–2.16 (m, 3H), 2.97–3.01 (m, 1H), 3.22–3.25(m, 4H), 3.63–3.71 (m, 1H), 3.76–3.90 (m, 5H), 4.37 (d, *J* = 5.5 Hz, 1H, H-11a), 6.90 (d, *J* = 8.8 Hz, 2H), 6.98 (d, *J* = 8.0 Hz, 1H), 7.16 (t, *J* = 8.1 Hz, 1H), 7.42 (t, *J* = 8.0 Hz, 1H), 7.70 (d, *J* = 8.8 Hz, 2H), 7.95 (d, *J* = 8.0 Hz, 1H), 8.40 (s, 1H, CH), 8.52 (s, 1H, NH); $^{13}$C-NMR (100 MHz, $CDCl_3$): δ = 23.6, 26.1, 47.4, 48.2, 55.5 (C-11a), 66.8, 114.7, 120.7, 123.6, 125.6, 126.3, 129.6, 131.5, 132.4, 137.0, 153.0, 156.7, 157.6, 166.1 (C=O); UV $\lambda_{max}$ (MeOH): 235, 350; IR (neat): 3259, 2956, 2854, 2350, 1706, 1619 (C=O), 1517, 1469, 1394, 1224, 1120, 927, 827, 759.82, 700; GC-MS (70 eV) *m/z* (%): 403 (1) [M+], 355 (8), 327 (9), 281 (49), 253 (20), 207 (100), 119 (16), 133 (12), 96 (13), 73 (20), 44 (50); HRMS m/z calcd for $C_{23}H_{25}N_5O_2$ $[M + H]^+$ 404.2087, found 404.2145.

#### (S,E)-11-[2-(2-thiophenylmethylene)hydrazono]-pyrrolo[2,1-c][1,4]benzodiazepine (4g)

Starting material 2-thiophenecarboxaldehyde (0.93 mL, 10 mmol) was used and the reaction mixture was stirred under nitrogen gas overnight for 15 h. The reaction mixture was then quenched with 20 mL of distilled water and filtered off. Crystallization from 2-propopanol gave a yellow crystalline solid of compound **4g**. Yield 788 mg (81.0%) mp 210–212 °C; $[\alpha]^{25}_D = +46°$ (*c* 0.5, $CHCl_3$); $^1$H-NMR (400 MHz, $CDCl_3$): δ = 1.95–2.18 (m, 3H), 2.95–3.02 (m, 1H), 3.674–3.71 (m, 1H), 3.75–3.83 (m, 1H), 4.34 (d, *J* = 5.4 Hz, 1H, H-11a), 6.98 (d, *J* = 8.1 Hz, 1H), 7.08 (t, *J* = 4.2 Hz, 1H), 7.16 (t, *J* = 8.2 Hz, 1H), 7.33 (d, *J* = 4.2 Hz, 1H), 7.37–7.45 (m, 2H), 7.95 (d, *J* = 8.0 Hz, 1H), 8.42 (s, 1H, NH), 8.58 (s, 1H, CH); $^{13}$C-NMR (100 MHz, $CDCl_3$): δ = 23.5, 26.1, 47.3, 55.45 (C-11a), 120.7, 123.7, 126.3, 127.7, 128.9, 131.2, 131.4, 132.2, 136.73, 139.7, 151.3, 157.1, 165.9 (C=O); UV $\lambda_{max}$ (MeOH): 215, 326; IR (neat): 3278, 2975, 2872, 2332, 1636 (C=O), 1582, 1395, 1221, 1093, 987, 752, 535; GC-MS (70 eV) *m/z* (%): 324 (100) [M+], 281(15), 241 (42), 207 (20), 160 (33), 145 (48), 119 (1257), 90 (26), 60 (29); HRMS m/z calcd for $C_{17}H_{17}N_4OS$ $[M + H]^+$ 325.1123, found 325.1115.

#### (S,E)-11-[2-(3-indolylmethylene)hydrazono]-pyrrolo[2,1-c][1,4]benzodiazepine (4h)

(*Tert*-butyl-3-formyl-1H-indole-1-carboxylate) methylene hydrazono PBD (460 mg, 1.0 mmol) was reacted with potassium carbonate (979 mg, 7.1 mmol) in a 20 mL mixture of MeOH/$H_2O$ and reflux for 30 min. The mixture was cooled down and washed with ether to afford white solids of compound 4 h. Yield 268 mg (75.0%) mp; 242–243 °C; $[\alpha]^{25}_D = +56°$ (*c* 0.5, $CHCl_3$): $^1$H-NMR (400 MHz, $CDCl_3$): δ = 1.94–2.03 (m, 3H), 2.81–2.88 (m, 1H), 3.54–3.67 (m, 2H), 4.46 (d, *J* = 5.1 Hz, 1H), 7.14–7.22 (m, 2H), 7.36 (d, *J* = 6.5 Hz, 1H), 7.50 (t, *J* = 8.1 Hz, 1H), 7.76 (d, *J* = 6.2 Hz, 1H), 7.95 (s, 1H, NH), 8.34 (d, *J* = 7.0 Hz, 1H), 8.66 (s, 1H, CH), 8.97 (s, 1H, NH); $^{13}$C-NMR (100 MHz, $CDCl_3$): δ = 23.66, 26.30, 47.44, 55.56 (C-11a), 112.65, 121.17, 122.40, 122.74, 123.01, 123.19, 131.02, 132.61, 137.97, 138.12, 153.92, 154.66, 165.63 (C=O). UV $\lambda_{max}$ (MeOH): 221, 331 nm. IR (KBr): 3504, 2917, 2850, 2337, 1751, 1617 (C=O), 1371, 1240, 1052, 877, 746, 608. GC-MS (70 eV) *m/z* (%): 357 (2) [M+], 355 (6), 327 (9), 281 (52), 253 (18), 249 (7), 207 (100), 191 (15), 177 (5), 133 (11), 119 (5), 96 (13), 73 (19), 44 (46); HRMS m/z calcd for $C_{21}H_{20}N_5O$ $[M + H]^+$ 358.1668, found 358.1653.

### Molecular modeling experimental part

The CB1 and CB2 crystal structures 5XRA and 5ZTY respectively were retrieved from protein data bank and prepared with MOE QuickPrep protocol. The docking procedure and visual analysis were performed using the standard protocol implemented in MOE 2018 (Chemical Computing Group, Montreal, Canada) [20]. The induced fit method was employed for refinement of the docked poses. Finally, the generated poses were ranked according to their docking scores. The ADMET properties were calculated in silico using ADMET predict 9 from Simulation Plus, Inc [21].

### Cannabinoid receptor binding assay

The affinities of the compounds for CB1 and CB2 receptors were examined using displacement assays, as previously described [22–24]. Briefly, cell membranes from CHO cells expressing human CB1 or human CB2 receptors were isolated using differential centrifugation. Test compounds reconstituted in DMSO and were incubated with the isolated membrane in binding buffer (50 mM Tris-HCl, 1 mM EDTA, 3 mM $MgCl_2$, 5 mg/mL BSA, pH 7.4) along with

2.5 nM [$^3$H]CP-55,940. Total binding was assessed in the presence of equal concentration of DMSO while non-specific binding was determined in the presence of 10 µM CP-55,940, and background binding was determined in wells lacking membrane. Following incubation at 30 °C for 60 min, the binding reactions will be terminated by filtration through Whatman GF/C filters. The filters will then be washed twice with ice-cold buffer (50 mM Tris-HCl, 1 mg/mL BSA). Liquid scintillation cocktail was added to each well and the total tritiated counts per minute were analyzed using a TopCount scintillation counter. Background counts were subtracted from all wells and the percent displacement from total binding was calculated.

The compounds were initially screened at 10 µM concentrations. If they produced at least ±30% displacement of the radioligand, then full competition curves was constructed. $K_i$ values were calculated using GraphPad Prism (San Diego, CA) and $K_d$ values determined using a 1 site fit. All assays were run in technical and biological replicates so that the $n = 5$–6.

## Results and discussion

### 1. Chemistry

A series of (*S*,*E*)-11-[2-(arylmethylene)hydrazono]-PBD analogs were synthesized via previously reported methods and new approaches in high yield. The synthesis of all PBD derivatives began from a readily available basic structure of PBD natural product from *Isatis indigotica*. As shown in (Fig. 2), the cyclocondensation of equimolar mixture of L-proline and isatoic anhydride in DMF at 155 °C afforded the dilactam **1**. Crystallization of dilactam **1** has been executed in 10:1 v/v mixture of acetone and DMF to obtain compound **1** as white crystals. Thionation of compound **1** with 0.5 equiv of 2,4-bis-(4-methoxyphenyl)-1,3-dithia-2,4-diphosphetane-2,4-disulfide (Lawesson's reagent) in THF at room temperature generated thiolactam **2**. Then treatment of **2** with hydrazine monohydrate in ethanol at room temperature afforded compound **3** which was further used as the core precursor for the synthesis of (*S*,*E*)-11-[2-(arylmethylene)hydrazono]-PBD analogs (**4a**–**4h**). The title compound **3** was subjected to condensation with several aldehydes in anhydrous MeOH and molecular sieves (3 Å) at room temperature to give a series of highly conjugated Schiff base **4** in high yield. Compound **4 h** was synthesized from the sequential condensation of **3** and *N*-Boc-protected-indole-3-carboxaldehyde via the Schiff base template condensation reaction followed by *N*-Boc deprotection in the presence of excess $K_2CO_3$. Upon further crystallization of crude product from EtOAc/hexanes, pure **4a**–**4h** were formed as crystalline solids.

### 2. Docking studies

#### A. Molecular docking with CB1

Herein we explore the plausible binding mode of **4b**, **4g** and **4h** into the orthosteric pocket of CB1 crystal structure (PDB:5XRA) [25]. This is a high resolution CB1 crystal structure with a synthetic full agonist AM11542, which takes an L-shape conformation inside the pocket (Fig. 3). The interactions between AM11542 and CB1 are mainly hydrophobic and aromatic; the tricyclic tetrahydrocannabinol ring system of AM11542 forms π–π interactions with Phe268, Phe379, Phe189, Phe170 and Phe177, and the phenolic hydroxyl at C1 forms a hydrogen bond with Ser383. Similar to AM11542, **4b** adopts an L-shape conformation in the orthosteric-binding pocket. Its interactions into CB1 are mainly hydrophobic and aromatic with residues embedded in the extracellular loop 2 [26, 27]. The tricyclic PBD ring system (the head) of **4b** forms π–π interactions with Phe108, Phe170, Phe179 and Phe379, and the ethylbenzene (the end-tail) maintain two interactions with Trp279 and Met363. On the contrary, **4g** and **4h** failed to occupy the pocket in the correct shape and did not form any significant intermolecular interaction with the critical

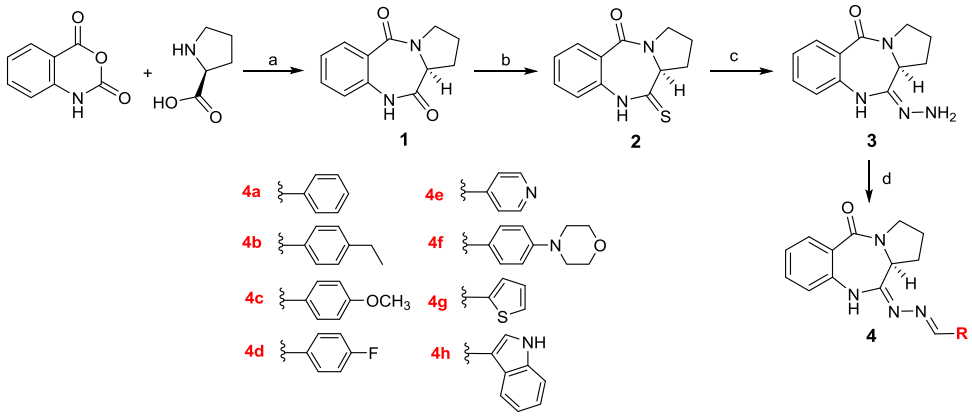


**Fig. 2** Reagents and conditions: (a) DMF, 155 °C, 5 h, 82.0%; (b) Lawesson's reagent, THF, rt, 15 h, 87.0%; (c) $N_2H_4.H_2O$ (98%), EtOH(abs.), rt, 15 h, 99.0%; (d) Aldehydes, MeOH (anhy.), rt, 15 h, 95.0%

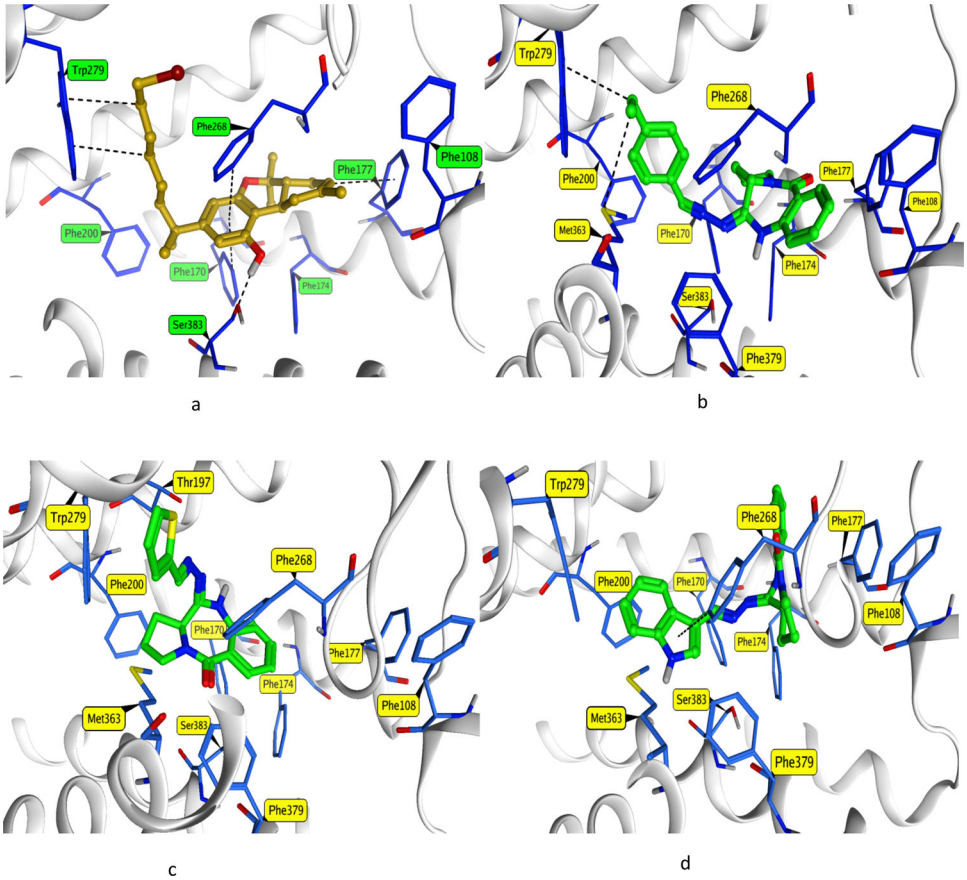


**Fig. 3** Binding modes of selected compounds into CB1 orthosteric-binding pocket. (**a**) Native ligand **AM11542** (yellow sticks) (**b**), (**c**) and (**d**) **4b**, **4g**, and **4h** (green sticks), respectively. Key amino acid residues shown as blue sticks; non-Carbon atoms are colored by element. Settled intermolecular interactions (black dotted lines). Some amino acids were hidden for clarity

amino acid residues denoting unfavorable binding. Only one H-π interaction between **4h** indole and Phe268 exists.

### B. Molecular docking with CB2

All previous modeling trials on CB2 were based on its homology model due to lack of its crystal structure. Primarily, we pursued a similar approach and constructed a valid CB2 model based on CB1 available crystal structure (42% sequence identity) [28]. However, during proceedings in the supposed workflow a high resolution co-crystalized CB2 structure with a highly active antagonist, AM10257, was revealed [29]. Although our model demonstrated an acceptable RMSD from CB2 crystal structure we preferred employing the latter for utmost accuracy [30]. The interactions between AM10257 and CB2 are mainly hydrophobic and aromatic with different hydrophobic amino acid residues in the pocket (Fig. 4-a). In addition, its terminal hydroxy group on the alkyl chain engages in a hydrogen bond. **4b** adopts a similar orientation where its PBD fragment maintains H-π interactions with both Phe183 and Tr194. The phenethyl moiety is buried in proximity to hydrophobic residues. **4g** and **4h** terminal chains have a similar orientation different from **4b**. The PBD of **4g** strongly interacts with Trp194 whereas its thiophene forms H-π interaction with Val113. **4h** terminal indole forges H-π interactions with the hydrophobic Phe87 and Phe183. The docking energy of **4b**, **4g**, and **4h** are similar (Table 1).

### C. ADMET properties

We evaluated the drug-likeness of promising CBs ligand by the computational calculation of ADMET and physicochemical properties (Table 2). In this regard, we computed various risks descriptors, such as absorption risk (Abs_Risk), risk associated with cytochrome P450 (CYP) enzymes (CYP_Risk), risk associated with various toxicity (TOX_Risk), ADMET_Risk, Lipinski's rules violations (Rule of 5) along with blood brain barrier penetration and retention (BBB filter and LogBB) [22]. Almost all of the predicted compounds possess Abs_risk, CYP_Risk, TOX_Risk, ADMET_Risk within the desired limit described by ADMET Predict tutorial by not exceeding 3.5, 2.5, 3.3, and 7.5, respectively. One exception is **4b** that may have a slightly higher toxicity value 3.33. All of the evaluated compounds obey all rules of Lipinski, which is a powerful indicator of good solubility, oral absorption, and permeability [23]. Those results imply that the designated compounds possess favorable drug-like properties.

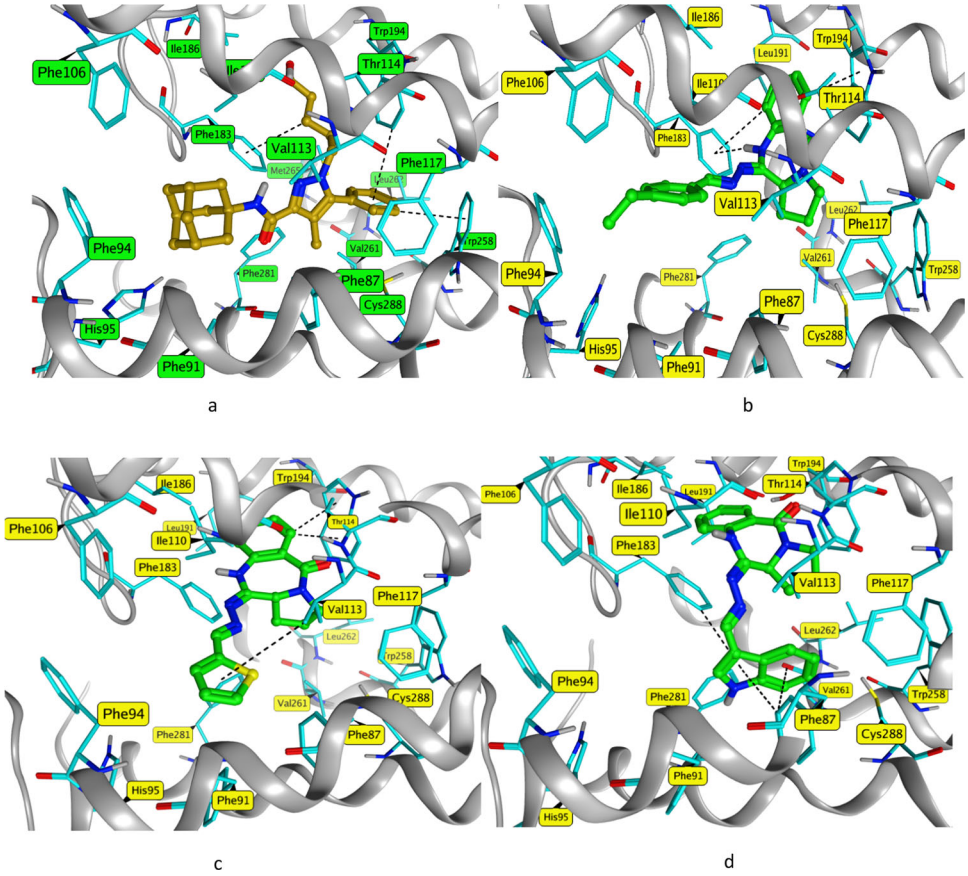


**Fig. 4** Binding modes of selected compounds into CB2 orthosteric-binding pocket. (**a**) Native ligand **AM10257** (yellow sticks), (**b**), (**c**) and (**d**) **4b**, **4g**, and **4h** (green sticks), respectively. Key amino acid residues shown as cyan sticks; non-Carbon atoms are colored by element. Settled intermolecular interactions (black dotted lines). Some amino acids were hidden for clarity

**Table 1** Binding energy of the docked compounds into CB1 and CB2 crystal structures (kcal/mol)

| Compound | CB1 | CB2 |
|---|---|---|
| **4a** | −6.2 | −5.9 |
| **4b** | −8.4 | −8.8 |
| **4c** | −8.4 | −8.6 |
| **4d** | −5.1 | −3.4 |
| **4e** | −6.8 | −7.9 |
| **4f** | −4.2 | −4.2 |
| **4g** | −3.9 | −8.8 |
| **4h** | −3.7 | −8.6 |

**4a** and **4c** exhibit a high possibility to cross BBB and work on CNS CB1 and they also have a moderate affinity toward CB2, which may lead to a non-selective pharmacological effect and undesirable adverse effects. On the contrary, **4b** is unlikely to bind CNS CB1 but it can bind CB2 and peripheral CB1. This can give rise to a promising CB2 modulator devoid of the psychoactive effects that are mediated by the CNS CB1 receptor. **4d** and **4f** are inactive CB1 and CB2 modulators. **4e** is a non-selective ligand that can pass BBB. **4g** and **4h** are highly selective CB2 modulators that if passed BBB may be expected not to elicit psychoactivity.

## 3. Biological evaluation of the synthesized compounds

The affinities of the compounds for CB1 and CB2 receptors were examined using displacement assays, as previously described [22–24]. PBD analogs **4a**–**4h** were investigated for CB1 and CB2 receptor binding properties by applying classical radioactivity-based assays. We carried out conventional radioligand binding assays using [$^3$H]CP55,940, which has low nanomolar affinities toward CB1 and CB2 receptors [31]. The results showed a weak to moderate radioligand displacement for **4a**, **4b**, **4c**, **4e**, **4g**, and **4h** at 10 μM, whereas no significant displacement was observed for **4d** and **4f** (Fig. 5). Compounds **4g** and **4h** were the most selective PBD analogs in displacement of [$^3$H]CP-55,940 radioligand. As shown in Fig. 5, **4g** and **4h** were able to partially displace [$^3$H]CP55,940 at CB2 receptors, but actually somewhat enhanced the binding at CB1. This unique displacement pattern suggests a likely allosteric, rather than competitive, binding interaction. An allosteric interaction between two ligands will occur when they bind to topographically distinct binding sites at the same

**Table 2** ADMET and physicochemical properties of active compounds calculated using ADMET Predictor 9.0; standard values are described at its tutorial

| Compound | Abs_risk | CYP_risk | TOX_risk | ADMET_risk | Rule of 5 | BBB filter | LogBB |
|---|---|---|---|---|---|---|---|
| **4a** | 0.00 | 1.00 | 3.00 | 4.00 | 0.00 | High | 0.27 |
| **4b** | 0.00 | 0.45 | 3.33 | 3.78 | 0.00 | Low | 0.05 |
| **4c** | 0.00 | 0.65 | 2.50 | 3.15 | 0.00 | High | 0.32 |
| **4d** | 0.00 | 1.00 | 3.04 | 4.04 | 0.00 | Low | −0.04 |
| **4e** | 0.147 | 0.34 | 3.00 | 3.48 | 0.00 | High | 0.23 |
| **4f** | 0.00 | 0.47 | 3.00 | 3.46 | 0.00 | High | 0.16 |
| **4g** | 0.00 | 0.03 | 3.00 | 3.30 | 0.00 | High | 0.17 |
| **4h** | 1.00 | 0.60 | 3.00 | 4.60 | 0.00 | High | 0.00 |

Abs_risk (Absorption risk) should not exceed 3.5

CYP_Risk (risk associated with cytochrome P450) should not exceed 2.5

TOX_Risk (Toxicity risk) should not exceed 3.3

ADMET_risk should not exceed 7.5

Rule of 5 predicts violation of Lipinski rule of 5

BBB filter predicts BBB penetration

Higher LogBB predicts greater likelihood of retention in the CNS.

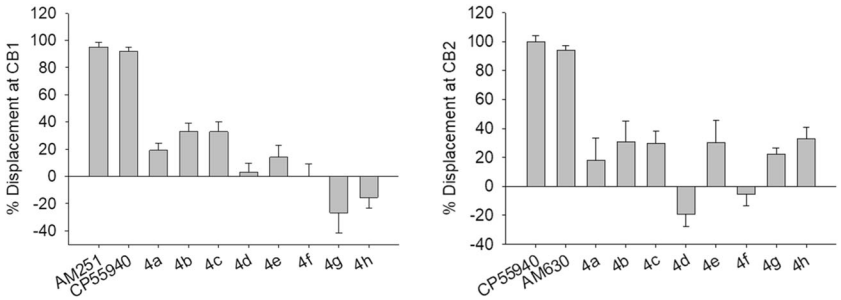


**Fig. 5** Binding affinities of compounds **4a**–**h** toward CB1 and CB2

receptor. Therefore, their full competition curves were constructed and their CB1/CB2 binding properties were further investigated toward CB2 in a concentration-dependent assay. Intriguingly, binding assay in various concentrations showed a selective binding affinity of **4g** and **4h** possessing $K_i$ values of 0.49 and 4.7 μM toward CB2 receptors while no binding was observed to CB1.

## Conclusion

This study highlights the design and synthesis of several (*S*,*E*)-11-[2-(arylmethylene)hydrazono]-PBD derivatives through a structure-based rational design using a multi-step synthesis approach to establish potential clusters of selective CB2 ligands. Beginning with computer-based docking studies, calculation of ADMET, and physicochemical properties, considering the calculation of BBB filter and LogBB, we prepared a series of PBD analogs as potential CB2 ligands and tested their binding affinities toward CB1/CB2.

The designed analogs have displayed potential binding efficacy toward CB1 and CB2 receptors tested. Among the designed analogs **4g** and **4h** showed $K_i$ of 0.49 and 4.7 μM toward CB2 receptors while no binding was observed toward CB1, which raise their potentiality as developed pharmacophore in targeting neurodegenerative disorders. The drug-likeness of the prepared ligands was calculated via computational calculation of ADMET and physicochemical properties. The generated data suggested that almost all the designed analogs possess Abs_risk, CYP_Risk, TOX_Risk, ADMET_Risk within the acceptable defined limits. The structural activity relationship (SAR) suggested the attachment of S- or N-heterocyclic aldehydes to the hydrazine part improves the selectivity of CB2 over CB1. This work has opened the window toward the development of more selective and potent CB2 ligands as preferred candidates for further biological evaluations.

**Acknowledgements** The authors are thankful to the Neuropharmacology CORE (CORE-NPN), School of Pharmacy, University of Mississippi for biological testing. The authors acknowledge the Department of Chemistry and The School of Graduate Studies at ETSU. This work is supported by the National Institute of General Medical Science of the National Institute of Health under Award Number P30GM122733. We are also grateful for the financial support of the ETSU Office of Research and Sponsored Programs Administration (ORSPA). The content is solely the responsibility of the authors

and does not necessarily represent the official views of the National Institutes of Health.

## Compliance with ethical standards

**Conflict of interest** The authors declare no conflict of interest.

**Publisher's note** Springer Nature remains neutral with regard to jurisdictional claims in published maps and institutional affiliations.

## References


1. Gao HM, Hong JS. Why neurodegenerative diseases are progressive: uncontrolled inflammation drives disease progression. Trends Immunol. 2008;29:357–65.
2. Brettschneider J, Tredici KD, Lee VM, Trojanowski JQ. Spreading of pathology in neurodegenerative diseases: a focus on human studies. Nat Rev Neurosci. 2015;16:109–20.
3. Sonkusare SK, Kaul CL, Ramarao P. Dementia of Alzheimer's disease and other neurodegenerative disorders—memantine, a new hope. Pharm Res. 2005;51:1–7.
4. McPartland JM. Phylogenomic and chemotaxonomic analysis of the endocannabinoid system. Brain Res Rev. 2004;45:18–29.
5. Ahn K, McKinney MK, Cravatt BF. Enzymatic pathways that regulate endocannabinoid signaling in the nervous system. Chem Rev. 2008;108:1687–707.
6. Aso E, Ferrer I. Cannabinoids for treatment of Alzheimer's disease: moving toward the clinic. Front Pharm. 2014;5:37.
7. Pacher P, Bátkai S, Kunos G. The Endocannabinoid System as an Emerging Target of Pharmacotherapy. Pharm Rev. 2006;58:389–462.
8. Dhopeshwarkar A, Mackie K. CB2 Cannabinoid receptors as a therapeutic target-what does the future hold? Mol Pharm. 2014;86:430–7.
9. Contino M, Capparelli E, Colabufo NA, Bush AI. Editorial: the CB2 Cannabinoid System: a new strategy in neurodegenerative disorder and neuroinflammation. Front Neurosci. 2017;11:196.
10. Lynn AB, Herkenham M. Localization of cannabinoid receptors and nonsaturable high-density cannabinoid binding sites in peripheral tissues of the rat: implications for receptor- mediated immune modulation by cannabinoids. J Pharm Exp Ther. 1994;268:1612–23.
11. Beltramo M, Bernardini N, Bertorelli R, Campanella M, Nicolussi E, Fredduzzi S, et al. CB2 receptor-mediated antihyperalgesia: possible direct involvement of neural mechanisms. Eur J Neurosci. 2006;23:1530–8.
12. Mukhopadhyay S, Das S, Williams EA, Moore D, Jones JD, Zahm DS. et al. Lypopolysaccharide and cyclic AMP regulation of CB2 cannabinoid receptor levels in rat brain and mouse RAW 264.7 macrophages. J Neuroimmunol. 2006;181:82–92.
13. Nakagawa Y, Chiba K. Role of microglial m1/m2 polarization in relapse and remission of psychiatric disorders and diseases. Pharmaceuticals. 2014;7:1028–48.
14. Aso E, Andres-Benito P, Carmona M, Maldonado R, Ferrer I. Cannabinoid receptor 2 participates in amyloid-beta processing in a mouse model of Alzheimer's disease but plays a minor role in the therapeutic properties of a cannabis-based medicine. J Alzheimers Dis. 2016;51:489–500.
15. Aso E, Juves S, Maldonado R, Ferrer I. CB2 cannabinoid receptor agonist ameliorates Alzheimer-like phenotype in AbetaPP/PS1 mice. J Alzheimers Dis. 2013;35:847–58.
16. Martin-Moreno AM, Brera B, Spuch C, Carro E, Garcia-Garcia L, Delgado M, et al. Prolonged oral cannabinoid administration prevents neuroinflammation, lowers beta-amyloid levels and improves cognitive performance in Tg APP 2576 mice. J Neuroinflamm. 2012;9:8.
17. Hebert LE, Weuve J, Scherr PA, Evans DA. Alzheimer disease in the United States (2010–250) estimated using the 2010 census. Neurology. 2013;80:1778–83.
18. Anavi-Goffer S, Gertsch J. Ariel University Research and Development Co Ltd, 2016. CB2 receptor ligands for the treatment of psychiatric disorders. U.S. Patent 9,486,419.
19. Cipolla L, Araújo AC, Airoldi C, Bini D. Pyrrolo[2,1-c][1,4] benzodiazepine as a scaffold for the design and synthesis of antitumour drugs. Anticancer Agents Med Chem. 2009;9:1–31.
20. El-Shaheny R, Radwan MO, Belal F, Yamada K. Pentabromobenzyl-RP versus triazole-HILIC columns for separation of the polar basic analytes famotidine and famotidone: LC method development combined with in silico tools to follow the potential consequences of famotidine gastric instability. J Pharm Biomed Anal. 2020;18:113305.
21. El-Shaheny R, Radwan M, Yamada K, El-Maghrabey M. Estimation of nizatidine gastric nitrosatability and product toxicity via an integrated approach combining HILIC, in silico toxicology, and molecular docking. J Food Drug Anal. 2019;27:915–25.
22. Lange JH, Coolen HK, van Stuivenberg HH, Dijksman JA, Herremans AH, Ronken E, et al. Synthesis, biological properties, and molecular modeling investigations of novel 3,4-diarylpyrazolines as potent and selective CB1 cannabinoid receptor antagonists. J Med Chem. 2004;47:627–43.
23. Papahatjis DP, Nikas SP, Kourouli T, Chari R, Xu W, Pertwee RG, et al. Pharmacophoric requirements for the cannabinoid side chain. Probing the cannabinoid receptor subsite at C1'. J Med Chem. 2003;46:3221–9.
24. Griffin G, Wray EJ, Tao Q, McAllister SD, Rorrer WK, Aung MM, et al. Evaluation of the cannabinoid CB2 receptor-selective antagonist SR144528: further evidence for cannabinoid CB2 receptor absence in the rat central nervous system. Eur J Pharm. 1999;377:117–25.
25. Hua T, Vemuri K, Nikas SP, Laprairie RB, Wu Y, Qu L, et al. Crystal structures of agonist-bound human cannabinoid receptor CB1. Nature. 2017;547:468–71.
26. Khan N, Halim SA, Khan W, Zafar SK, Ul-Haq Z. In-silico designing and characterization of binding modes of two novel inhibitors for CB1 receptor against obesity by classical 3D-QSAR approach. J Mol Graph Model. 2019;1:199–214.
27. Kumar KK, Shalev-Benami M, Robertson MJ, Hu H, Banister SD, Hollingsworth SA, et al. Structure of a signaling cannabinoid receptor 1-G protein complex. Cell. 2019;176:448–58.
28. Shao Z, Yin J, Chapman K, Grzemska M, Clark L, Wang J, et al. High-resolution crystal structure of the human CB1 cannabinoid receptor. Nature. 2016;540:602–6.
29. Li X, Hua T, Vemuri K, Ho JH, Wu Y, Wu L, et al. Crystal structure of the human cannabinoid receptor CB2. Cell. 2019;176:459–67.
30. Porter RF, Szczesniak AM, Toguri JT, Gebremeskel S, Johnston B, Lehmann C, et al. Selective Cannabinoid 2 Receptor Agonists as Potential Therapeutic Drugs for the Treatment of Endotoxin-Induced Uveitis. Molecules. 2019;24:3338.
31. Pertwee RG, Howlett AC, Abood ME, Alexander SP, Di Marzo V, Elphick MR, et al. International Union of Basic and Clinical Pharmacology. LXXIX. Cannabinoid receptors and their ligands. Beyond CB1 and CB2. Pharm Rev. 2010;62:588–631.

## Affiliations

David Mingle[1] · Meirambek Ospanov[2] · Mohamed O. Radwan[3,4,5] · Nicole Ashpole[6] · Masami Otsuka[3,4] · Samir A. Ross[2,6] · Larry A. Walker[2] · Abbas G. Shilabin[1] · Mohamed A. Ibrahim[2,5]

[1] Department of Chemistry, East Tennessee State University, Johnson City, TN 37614, USA

[2] National Center for Natural Products Research, School of Pharmacy, University of Mississippi, University, MS 38677, USA

[3] Medicinal and Biological Chemistry Science Farm Joint Research Laboratory, Kumamoto University, Kumamoto 862-0973, Japan

[4] Department of Drug Discovery, Science Farm Ltd., Kumamoto 862-0976, Japan

[5] Chemistry of Natural Compounds Department, Pharmaceutical and Drug Industries Research Division, National Research Centre, Dokki, Cairo 12622, Egypt

[6] Department of BioMolecular Sciences, School of Pharmacy, University of Mississippi, University, MS 38677, USA